Uncertainty Quantification of Fiber Orientation and Epicardial Activation

Lindsay C Rupp[1,2,3], Anna Busatto[1,2,3], Jake A Bergquist[1,2,3], Karli Gillette[5], Akil Narayan[1,4], Gernot Plank[5], Rob S MacLeod[1,2,3]

[1] Scientific Computing and Imaging Institute, University of Utah, SLC, UT, USA
[2] Nora Eccles Cardiovascular Research and Training Institute, University of Utah, SLC, UT, USA
[3] Department of Biomedical Engineering, University of Utah, SLC, UT, USA
[4] Department of Mathematics, University of Utah, SLC, UT, USA
[5] Institute of Biophysics, Medical University of Graz, Graz, Austria

Abstract

Predictive models and simulations of cardiac function require accurate representations of anatomy, often to the scale of local myocardial fiber structure. However, acquiring this information in a patient-specific manner is challenging. Moreover, the impact of physiological variability in fiber orientation on simulations of cardiac activation is poorly understood. To explore these effects, we implemented bi-ventricular activation simulations using rule-based fiber algorithms and robust uncertainty quantification techniques to generate detailed maps of model variability. Specifically, we utilized polynomial chaos expansion, enabling efficient exploration with reduced computational demand through an emulator function approximating the underlying forward model. Our study focused on examining the epicardial activation sequences of the heart in response to six stimuli locations and five metrics of activation. Our findings revealed that physiological variability in fiber orientation does not significantly affect the location of activation features, but it does impact the overall spread of activation. We observed low variability near the earliest activation sites, but high variability across the rest of the epicardial surface. We conclude that the level of accuracy of myocardial fiber orientation required for simulation depends on the specific goals of the model and the related research or clinical goals.

1. Introduction

Personalized computational models play an increasingly important role as a reliable approach to studying the mechanisms of cardiac arrhythmias and treatment strategies. [1] One crucial component of personalized modeling is accurately representing cardiac anatomy and local myocardial fiber orientation to create the digital twin. Common approaches to capturing this information include image-based acquisition and rule-based algorithms. [2, 3] In either method, fiber directions contain errors, the impacts of which are incompletely understood. Physiological variability of up to 20 $^\circ$ also exists on the epicardial and endocardial surfaces. [4] The impacts of such variability on the predicted spread of electrical activation also remain largely unknown.

The effect of variable fiber orientation on myocardial activation sequences has been reported; however, these studies lacked comprehensive statistical analysis. [5, 6] Many methods exist for simulation-based uncertainty assessment, such as Monte Carlo or range-finding techniques. A more sophisticated uncertainty quantification (UQ) technique is non-intrusive polynomial chaos expansion (PCE) methods. Non-intrusive PCE methods use advanced sampling methods to exploit structure in stochastic fields or processes of interest to reduce the requisite computational demand for obtaining accurate statistics. [7]

In this study, we simulated cardiac activation from ventricular-paced beats using an Eikonal model, rule-based fiber orientations, and robust uncertainty quantification algorithms to capture detailed maps of model sensitivity. Overall, for all six stimuli locations, two trends emerged: (1) epicardial stimuli generate activation sequences with **higher levels of variability** than endocardial stimuli, and (2) endocardial stimuli produce sequences with **increased areas of variability**. Furthermore, we observed low variability for the earliest and latest activation sites but high variability for the orientation and area of the breakthrough site. In summary, the responses to uncertainty in fiber direction depended on both stimulus parameters and the output metrics of interest.

2. Methods

Biventricular geometric models were generated from magnetic resonance images of explanted porcine hearts in

the form of finite-element meshes (edge length, 700 μm). [8] Activation sequences were computed with CARPentry using an Eikonal model. [9] We examined the spread of activation in response to the uncertainty in fiber orientation using six stimulation locations: epicardial and endocardial apex, epicardial and endocardial left ventricular free wall, and epicardial and endocardial right ventricular free wall. All locations were prescribed automatically using universal ventricular coordinates. [10, 11]

The rule-based fiber algorithm assumed a linear rotation of the fiber angle α and helix angle β from the endocardium to the epicardium. [3] The baseline epicardial and endocardial fibers were set to -60° (α_{epi}) and 60° (α_{endo}), respectively, and the helix epicardial and endocardial fibers were set to 0° (β_{epi}) and -35° (β_{endo}), respectively. [4] We altered α_{epi} and α_{endo} uniformly between -35 to -85° and 35 to 85°, respectively. [4]

We quantified the effects of uncertainty in the fiber orientation using PCE via the open-source software UncertainSCI. [7] UncertainSCI used a polynomial function emulator of degree five (31 samples) to approximate the underlying forward model. The statistical response, mean, and standard deviation (STD) were calculated for epicardial projections of the activation sequence. In addition, we analyzed five activation metrics: (1) the total activation time, (2) the location of the earliest epicardial activation (breakthrough) for the endocardial left and right ventricular free wall stimuli, (3) the location of the latest activation, (4) the orientation of the breakthrough site isochrone (10% of epicardial total activation time) for the epicardial and endocardial left ventricular free wall stimuli, and (5) the area of the breakthrough site isochrone for all stimuli except the endocardial apex. [12] To determine the orientation of the breakthrough isochrone, we projected its three-dimensional shape onto a plane, and used a set of conic equations to fit an ellipse to these projected points.

3. Results

Figure 1A shows the mean and STD activation times for epicardial and endocardial **apex** stimuli. For both stimuli, the STD values were lower ($\leq$ 0.8 ms) near the stimulus and higher ($\leq$ 6.4 ms) near the base of the heart. Figure 1B shows the equivalent results for the **left ventricular free wall** stimuli. For the epicardial stimulus, the STD values were higher ($\leq$ 8.3 ms) near flanking regions of the breakthrough site and lower ($\simeq$ 0 ms) at the breakthrough and termination sites. For the endocardial stimulus, the STD patterns were more complex than the epicardial stimulus. Specifically, the variability was higher ($\leq$ 4.4 ms) near flanking regions of the breakthrough site and lower ($\leq$ 0.1 ms) STD at the breakthrough. Figure 1C shows the results for **right ventricular free wall** stimuli; the epicardial stimulus showed similar patterns, relative to the stimulation site, as the epicardial left ventricular free wall stimuli. As before, the variability was higher ($\leq$ 6.1 ms) near flanking regions of the breakthrough site and lower ($\leq$ 0.3 ms) STD values near the breakthrough sites. However, the endocardial stimulus differed, such that the left ventricular free wall had higher STD near the base of the heart, and the right ventricular free wall had higher STD near the apex of the heart.

The variability in fiber orientation produced high STDs of activation time compared to the total activation time, ranging between 3.2–8.8%. The location of the earliest activation site changed only minimally in response to variable fiber fields, with an STD range of 0.05–1.12 mm. Similarly, the latest activation site had low STDs: 0.02–9.33 mm. The orientation of the breakthrough site with respect to the short axis of the heart following LV stimulation was -51.2 $\pm$ 14.2°for an epicardial stimulus and 27.0 $\pm$ 12.8°for an endocardial. The minimum STD values for the area of the breakthrough site were 7.7 mm^2 and 44.4 mm^2 for epicardial and endocardial stimuli, respectively. The equivalent maximum STDs were 27.2 mm^2 and 75.5 mm^2, respectively.

4. Discussion

Predictive models and simulations of cardiac function require accurate representations of anatomy, often to the scale of local myocardial fiber structure. This study aimed to evaluate the role of fiber orientation on epicardial activation sequences using robust UQ. We implemented biventricular Eikonal simulations, rule-based fiber algorithms, and PCE techniques to capture detailed quantitative results. [3,7] Our findings suggest that fiber orientation has a minimal role in the location of discrete activation features but creates substantial variability in the overall spread of activation.

We observed for all stimuli that the baseline and mean activation sequences had similar activation time patterns and ranges (not shown), indicative of an underlying linear relationship between fiber orientation and epicardial activation. Overall, for all six stimulus sites, two trends emerged: (1) epicardial stimuli generate beats with overall higher STDs, and (2) endocardial stimuli produce overall increased surface areas of higher STD.

For the activation sequence metrics, we observed overall low variability in the locations of earliest and latest activation. However, the orientation of breakthrough isochrone showed high variability; furthermore, the epicardial stimuli produced higher STD values than the endocardial stimuli. These results are not surprising because an epicardial stimulus travels only a short distance before reaching the epicardial surface, and the orientation of the breakthrough region closely follows that of the superficial epicardial fibers. However, waves from endocardial stimuli

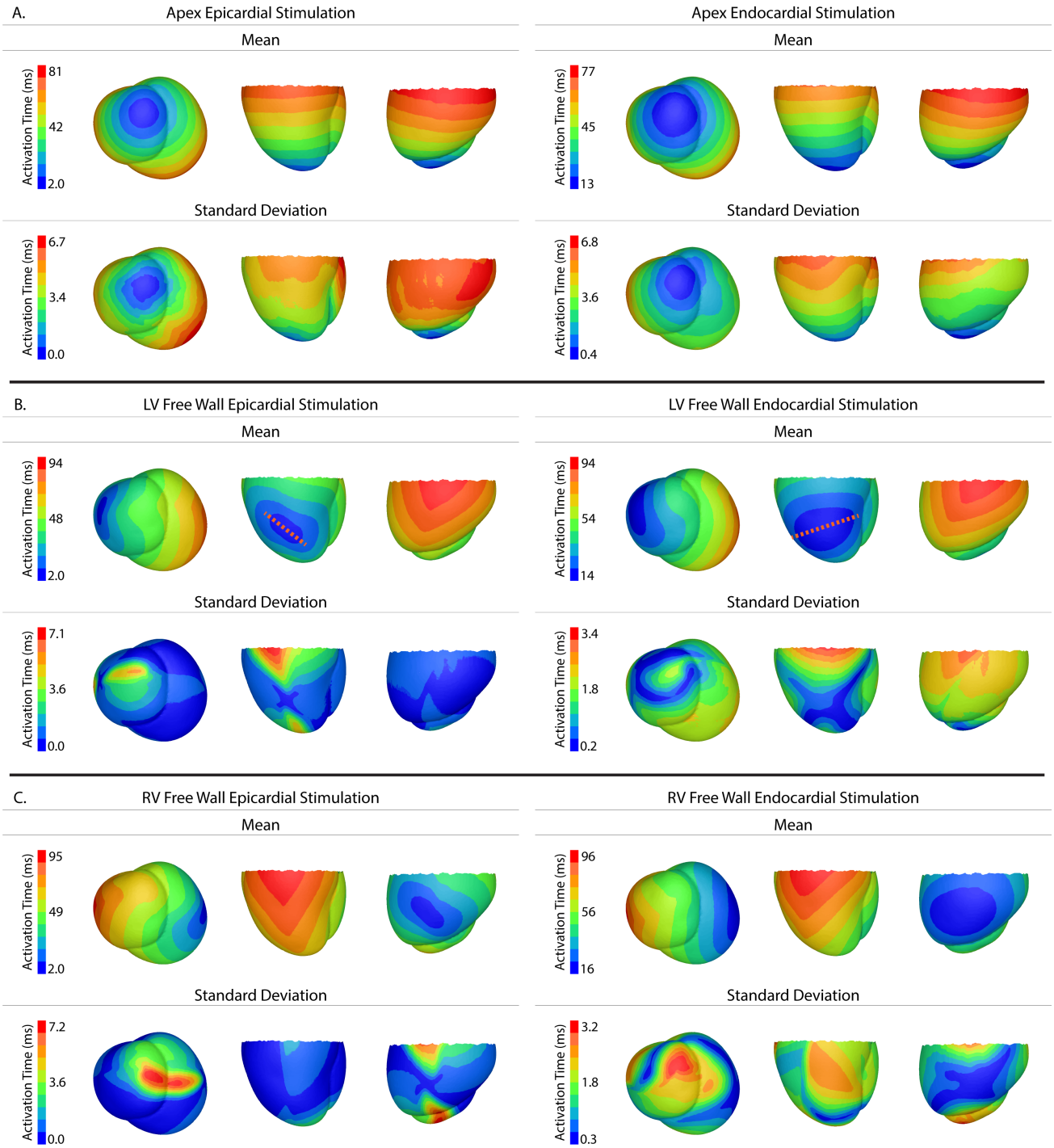

Figure 1: Uncertainty quantification of epicardial activation sequences. The top panel (A) shows the epicardial activation times for epicardial (left) and endocardial (right) apex stimuli locations. The middle panel (B) shows the activation sequence for epicardial (left) and endocardial (right) left ventricular free wall stimuli locations. The bottom panel (C) shows the activation sequence for epicardial (left) and endocardial (right) right ventricular free wall stimuli locations. For each panel, row one shows the mean activation sequence and row two shows the standard deviation of the activation sequence. Each panel shows views from three perspectives along the long axis of the heart: apical, left lateral, and right lateral side. The orange line(s) in panel B are an approximation of the breakthrough site orientation.

travel much further through a rotating fiber field before reaching the epicardial surface, thus experiencing rotation and smoothing. The longer pathway makes them more susceptible to variations in fiber orientation than epicardially paced beats. The area of breakthrough isochrones showed high variability, and the endocardial stimuli produced higher STD values than the epicardial stimuli, the opposite trend from the breakthrough site orientation. [12]

Because we focused on activation sequences, we selected the Eikonal simplification, but such a model lacks curvature effects [13]. A further limitation came from the analysis being applied to a single geometry and polynomial degree; however, we have explored both parameter spaces and found them to yield similar results. Lastly, we implemented rule-based fiber orientations, which can be seen as both a limitation and a strength. Rule-based algorithms are imperfect; however, they represent a parameterized description of fiber orientation, allowing us to impose a controlled range of fiber orientations; subject-specific fiber orientations lack such control. [3]

Our findings suggest that uncertainties in fiber orientation are unlikely to significantly affect clinical procedures that depend on identifying sites of early activation, such as the localization of focal arrhythmias. However, we did observe high variability throughout the spread of activation, which could potentially impact the modeling of reentrant arrhythmias, resulting in differences in the site or even the existence of re-entry. The effects on computed extracellular potentials and ECGs could also be substantial, with profound impacts on ECG imaging and localization of arrhythmias from the body surface. Future studies will explore a broader range of arrhythmias to improve our understanding of fiber orientation variability in predicting and localizing abnormal electrical activity in the heart.

Acknowledgments

Support for this research came from the Center for Integrative Biomedical Computing (www.sci.utah.edu/cibc), grants P41 GM103545, R24 GM136986, and U24EB029012, the NSF GRFP, and the Nora Eccles Harrison Foundation for Cardiovascular Research.

References

[1] Niederer SA, Lumens J, Trayanova NA. Computational models in cardiology. Nature reviews cardiology 2019; 16(2):100–111.

[2] Hsu EW, Henriquez CS. Myocardial fiber orientation mapping using reduced encoding diffusion tensor imaging. Journal of cardiovascular magnetic resonance 2001; 3(4):339–347.

[3] Bayer JD, Blake RC, Plank G, Trayanova NA. A novel rule-based algorithm for assigning myocardial fiber orientation to computational heart models. Annals of biomedical engineering 2012;40(10):2243–2254.

[4] Lombaert H, Peyrat JM, Croisille P, Rapacchi S, Fanton L, Cheriet F, Clarysse P, Magnin I, Delingette H, Ayache N. Human atlas of the cardiac fiber architecture: Study on a healthy population. IEEE transactions on medical imaging 2012;31(7):1436–1447.

[5] Konukoglu E, Relan J, Cilingir U, Menze BH, Chinchapatnam P, Jadidi A, Cochet H, Hocini M, Delingette H, Jaïs P, et al. Efficient probabilistic model personalization integrating uncertainty on data and parameters: Application to eikonal-diffusion models in cardiac electrophysiology. Progress in biophysics and molecular biology 2011; 107(1):134–146.

[6] Quaglino A, Pezzuto S, Koutsourelakis PS, Auricchio A, Krause R. Fast uncertainty quantification of activation sequences in patient-specific cardiac electrophysiology meeting clinical time constraints. International journal for numerical methods in biomedical engineering 2018; 34(7):e2985.

[7] Narayan A, Liu Z, Bergquist JA, Charlebois C, Rampersad S, Rupp L, Brooks D, White D, Tate J, MacLeod RS. UncertainSCI: Uncertainty quantification for computational models in biomedicine and bioengineering. Computers in biology and medicine 2023;152:106407.

[8] Zenger B, Good W, Bergquist J, Burton B, Tate J, Berkenbile L, Sharma V, MacLeod R. Novel experimental model for studying the spatiotemporal electrical signature of acute myocardial ischemia: A translational platform. J Physiol Meas Feb 2020;41(1):015002.

[9] Vigmond E, Santos RWD, Prassl A, Deo M, Plank G. Solvers for the cardiac bidomain equations. Progress in biophysics and molecular biology 2008;96(1):3–18.

[10] Bayer J, Prassl AJ, Pashaei A, Gomez JF, Frontera A, Neic A, Plank G, Vigmond EJ. Universal ventricular coordinates: A generic framework for describing position within the heart and transferring data. Medical image analysis 2018;45:83–93.

[11] Gillette K, Gsell MA, Prassl AJ, Karabelas E, Reiter U, Reiter G, Grandits T, Štern Darko, Urschler M, Bayer J, Augustin CA, Neic AV, Pock T, Vigmond EJ, Plank G. A framework for the generation of digital twins of cardiac electrophysiology from clinical 12-leads ECGs. Medical image analysis 2021;.

[12] Taccardi B, Punske BB, Macchi E, MacLeod RS, Ershler PR. Epicardial and intramural excitation during ventricular pacing: Effect of myocardial structure. American journal of physiology heart and circulatory physiology 2008; 294(4):H1753–H1766.

[13] Neic A, Campos FO, Prassl AJ, Niederer SA, Bishop MJ, Vigmond EJ, Plank G. Efficient computation of electrograms and ECGs in human whole heart simulations using a reaction-eikonal model. Journal of computational physics 2017;346:191–211.

Address for correspondence:

Name: Lindsay Cecala Rupp

Full postal address: SCI Institute, University of Utah, 72 Central Campus Dr, Salt Lake City, UT 84112

E-mail address: lindsay.rupp@utah.edu